The current issue and full text archive of this journal is available at
www.emeraldinsight.com/0961-5539.htm

Received 11 June 2007
Revised 10 March 2008
Accepted 19 March 2008

Effects of injection (suction) on a steady mixed convection boundary layer flow over a vertical cone

R. Ravindran
Centre for Differential Equations, Continuum Mechanics and Applications, School of Computational and Applied Mathematics, University of the Witwatersrand, Johannesburg, South Africa
Satyajit Roy
Department of Mathematics, Indian Institute of Technology Madras, Chennai, India, and
E. Momoniat
Centre for Differential Equations, Continuum Mechanics and Applications, School of Computational and Applied Mathematics, University of the Witwatersrand, Johannesburg, South Africa

Abstract

Purpose – The purpose of this paper is to study the steady mixed convection flow over a vertical cone in the presence of surface mass transfer when the axis of the cone is inline with the flow.
Design/methodology/approach – In this case, the numerical difficulties to obtain the non-similar solution are overcome by applying an implicit finite difference scheme in combination with the quasilinearization technique.
Findings – Numerical results are reported here to display the effects of Prandtl number, buoyancy and mass transfer (injection and suction) parameters at different stream-wise locations on velocity and temperature profiles, and on skin friction and heat transfer coefficients.
Research limitations/implications – Thermo-physical properties of the fluid in the flow model are assumed to be constant except the density variations causing a body force term in the momentum equation. The Boussinesq approximation is invoked for the fluid properties to relate the density changes to temperature changes and to couple in this way the temperature field to the flow field.
Practical implications – Convective heat transfer over a stationary cone is important for the thermal design of various types of industrial equipments such as heat exchangers, conisters for nuclear waste disposal, nuclear reactor cooling systems and geothermal reservoirs, etc.
Originality/value – The combined effects of thermal diffusion and surface mass transfer on a vertical cone has been studied.
Keywords Convection, Mass transfer, Flow, Boundary layers
Paper type Research paper

Nomenclature

A	surface mass transfer parameter
C_f	local skin friction coefficient
C_p	specific heat at constant pressure
f,F	dimensionless stream function and axial velocity component, respectively
g	acceleration due to gravity
G	dimensionless temperature
Gr_x	local Grashof number

International Journal of Numerical Methods for Heat & Fluid Flow
Vol. 19 Nos. 3/4, 2009
pp. 432-444

0961-5539
DOI 10.1108/09615530910938362

k thermal conductivity

m exponent in the power law variation of the free stream velocity

Nu local Nusselt number

Pr Prandtl number

Re_x local Reynolds number

T temperature

u axial velocity component

u_∞ free stream velocity

v radial velocity component

x axial coordinate

y transverse coordinate

Greek letters

β volumetric coefficient of thermal expansion

γ half angle of the vertical cone

ξ similarity variable

η similarity variable

λ buoyancy parameter

μ dynamic viscosity

ν kinematic viscosity

ρ density

ψ stream function

Subscripts

ω, ∞ conditions at the wall and infinity, respectively

ξ, η denote the partial derivatives with respect to these variables, respectively

1. Introduction

Most of the steady mixed convection boundary layer flow problems appearing in recent past demand detailed analysis taking non-similarity into account. The non-similarity in such flows may be due to curvature of the body or due to surface mass transfer (suction or injection), or even possibly due to all these effects. Convective heat transfer over a stationary cone is important for the thermal design of various types of industrial equipments such as heat exchangers, conisters for nuclear waste disposal, nuclear reactor cooling systems and geothermal reservoirs, etc. In recent years, several investigators have reported studies on natural and mixed convection flows over various geometries such as obstructed channels by Cruchaga and Celentano (2003), vertical surfaces by Lok *et al.* (2005), horizontal cylinders by Nazar *et al.* (2003), Ventilated cavities by Raji and Hasnaoui (2000), vertical plate by Rama Subba Reddy Gorla *et al.* (1998), rectangular enclosure by Anwar Hossain and Rama Subba Reddy Gorla (2006), rotating cone by Dijk *et al.* (2001), vertical cone by Pop *et al.* (2003) and vertical circular cone by Hossain *et al.* (2002).

In an early study, Hering and Grosh (1963) investigated the practical case of steady mixed convection from a vertical cone for $Pr = 0.7$. In a further study, Himasekhar *et al.* (1989) found the similarity solution of the mixed convection flow over a vertical rotating cone in an ambient fluid for a wide range of Prandtl numbers. Wang (1990) has obtained a similarity solution of boundary layer flows on rotating cone, discs and axisymmetric bodies with concentrated heat sources. Further, combined free and forced convection boundary layer flows over stationary and rotating vertical cylinders have been studied in detail, respectively, by Mahmood and Merkin (1988), Daskalakis (1993) and Pop *et al.* (1989). In contrast, Kumari *et al.* (1989) and Yih (1999) have presented numerical solutions to study the heat transfer characteristics in mixed convection flows from a vertical cone without and with porous media, respectively. In many practical problems, there are several transport processes with surface mass transfer (i.e. injection or suction) in industry where the buoyancy force arises from

thermal diffusion caused by temperature gradient. Therefore as a step towards the eventual development on steady mixed convection flows, it is interesting as well as useful to investigate the combined effects of thermal diffusion and surface mass transfer on a vertical cone.

The objective of the present analysis is to obtain non-similar solution of a steady mixed convection flow over a vertical cone with surface mass transfer (injection or suction). Non-similar solutions are obtained numerically by solving a set of coupled non-linear partial differential equations using an implicit finite difference scheme in combination with the quasilinearization technique. Particular cases of the present results have been compared with those of Hering and Grosh (1963), Himasekhar *et al.* (1989) and Kumari *et al.* (1989).

2. Analysis

Consider a vertical circular cone with a half angle γ along which a forced flow moves parallel to the axis of the cone with temperature T_∞. The surface of the cone is at a uniform higher temperature T_w, that is $T_w > T_\infty$ and the forced flow is in upward direction. The streamwise coordinate x is measured from the apex of the cone along its generator, and the transverse coordinate y is measured normal to it into the fluid, respectively (see Figure 1). Thermo-physical properties of the fluid in the flow model are assumed to be constant except the density variations causing a body force term in the momentum equation. The Boussinesq approximation is invoked for the fluid properties to relate the density changes to temperature changes and to couple in this way the temperature field to the flow field. Under the above assumptions and imposing Mangler's transformation to reduce the axi-symmetric problem into a two-dimensional problem (Schlichting, 2000), the continuity, momentum and energy equations governing steady mixed convection flow along a vertical cone can be written as

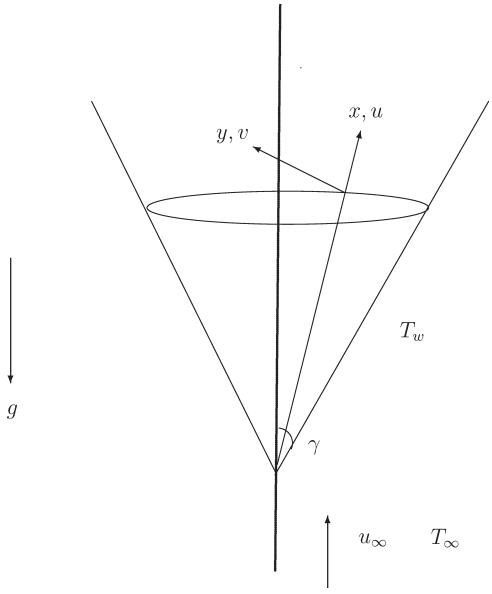

Figure 1.
Physical model and co-ordinate system

(Yih, 1999; Pop and Ingham, 2001; Bejan, 2004),

$$\frac{\partial u}{\partial x}+\frac{\partial v}{\partial y}=0, \tag{1}$$

$$u\frac{\partial u}{\partial x}+v\frac{\partial u}{\partial y}=U_e\frac{\partial U_e}{\partial x}+\nu\frac{\partial^2 u}{\partial y^2}+g\beta\cos\gamma(T-T_\infty), \tag{2}$$

$$u\frac{\partial T}{\partial x}+v\frac{\partial T}{\partial y}=\frac{\nu}{Pr}\frac{\partial^2 T}{\partial y^2}. \tag{3}$$

The boundary conditions are given by

$$\begin{aligned} u(x,0)&=0, \quad v(x,0)=v_w(x),\\ T(x,0)&=T_w=\text{Constant},\\ u(x,\infty)&=U(x)=u_\infty x^m,\\ T(x,\infty)&=T_\infty=\text{Constant}. \end{aligned} \tag{4}$$

Applying the following transformations

$$\begin{aligned} \eta&=y\left(\frac{m+1}{2}\frac{U}{\nu x}\right)^{1/2}, \quad \xi=\left(\frac{2}{m+1}\frac{\nu x}{U}\right)^{1/2},\\ \psi(x,y)&=\left(\frac{2}{m+1}\nu x U\right)^{1/2}f(\xi,\eta), \quad u=\frac{\partial\psi}{\partial y},\\ v&=-\frac{\partial\psi}{\partial x}, f_\eta(\xi,\eta)=F(\xi,\eta), \quad u=UF(\xi,\eta),\\ v&=-2^{-1}\left(\frac{2}{m+1}\frac{\nu U}{x}\right)^{1/2}[(m+1)f+(1-m)\ (\xi f_\xi-\eta F)],\\ G(\xi,\eta)&=\frac{T-T_\infty}{T_w-T_\infty}, \end{aligned} \tag{5}$$

to Equations (1)-(3), it is found that Equation (1) is satisfied identically, and Equations (2)-(3) reduce to

$$F_{\eta\eta}+fF_\eta+\frac{2m}{m+1}(1-F^2)+\frac{2}{m+1}\ \lambda G=\left(\frac{1-m}{m+1}\right)\xi(FF_\xi-F_\eta f_\xi), \tag{6}$$

$$Pr^{-1}G_{\eta\eta}+fG_\eta=\left(\frac{1-m}{m+1}\right)\xi(FG_\xi-G_\eta f_\xi), \tag{7}$$

where

$$\mathrm{Pr}=\frac{\mu C_p}{k},\ \mathrm{Gr_x}=\frac{g\beta x^3(T_w-T_\infty)\cos\gamma}{\nu^2},\ \mathrm{Re_x}=\frac{Ux}{\nu}\ \text{ and }\lambda=\frac{\mathrm{Gr_x}}{\mathrm{Re_x^2}}.$$

It may be noted that for $m = 1/2$, λ becomes a constant and numerical solutions are computed for different values λ as discussed in results and discussion section. Here ξ, η are the transformed co-ordinates; η_∞ is the edge of the boundary layer; ψ and f are dimensional and dimensionless stream functions, respectively; F and G are, respectively, dimensionless velocity and temperature.

The boundary conditions reduce to

$$\begin{aligned} F(\xi, 0) = 0, \quad G(\xi, 0) = 1 \quad \text{at} \quad \eta = 0, \\ F(\xi, \eta_\infty) = 1, \quad G(\xi, \eta_\infty) = 0 \quad \text{at} \quad \eta = \eta_\infty, \end{aligned} \tag{8}$$

where $f = \int_0^\eta F d\eta + f_w$ and f_w is given by

$$f_w + \left(\frac{1-m}{m+1}\right)\xi (f_\xi)_w = -\left(\frac{v_w}{\nu}\right)\xi = A\xi; \quad A = -\frac{v_w}{\nu}. \tag{9}$$

The surface mass transfer parameter $A > 0$ or $A < 0$ according to whether there is a suction or injection. It may be noted that the Equations (6) and (7) with $\xi = 0$, $\lambda = 0$ and $m = 0$ in the present problem are the same as those of Kumari *et al.* (1989).

The quantities of physical interest are as follows (Pop and Ingham, 2001; Bejan, 2004).

The local skin friction coefficient is given by

$$C_f = \frac{2[\mu(\partial u/\partial y)]_w}{\rho U^2} = 2(Re_x)^{-(1/2)}\left(\frac{m+1}{2}\right)^{1/2}(F_\eta)_w.$$

Thus,

$$Re_x^{1/2} C_f = 2\left(\frac{m+1}{2}\right)^{1/2}(F_\eta)_w \tag{10}$$

The local heat transfer rate at the wall in terms of Nusselt number can be expressed as

$$Re_x^{-(1/2)} Nu = -\left(\frac{m+1}{2}\right)^{1/2}(G_\eta)_w, \tag{11}$$

where $Nu = -([x(\partial T/\partial y)]_w)/(T_w - T_\infty)$.

3. Method of solution

The set of non-linear coupled partial differential equations (6) and (7) along with the boundary conditions (8), represent a non-linear two point boundary value problem for partial differential equations which is solved by an implicit finite difference scheme in combination with the quasilinearization technique (Bellman and Kalaba, 1965; Singh and Roy, 2007). Applying quasilinearization technique (Bellman and Kalaba, 1965; Singh and Roy, 2007), the non-linear coupled partial differential equations (6)-(7) are replaced by the following sequence of linear partial differential equations

$$F_{\eta\eta}^{i+1} + X_1^i F_\eta^{i+1} + X_2^i F^{i+1} + X_3^i F_\xi^{i+1} + X_4^i G^{i+1} = X_5^i \tag{12}$$

$$G_{\eta\eta}^{i+1} + Y_1^i G_\eta^{i+1} + Y_2^i G_\xi^{i+1} + Y_3^i F^{i+1} = Y_4^i \tag{13}$$

The coefficient functions with iterative index i are known and the functions with iterative index $i+1$ are to be determined. The boundary conditions become

$$\begin{aligned} F^{i+1} = 0, \quad G^{i+1} = 1 \quad \text{at} \quad \eta = 0, \\ F^{i+1} = 1, \quad G^{i+1} = 0 \quad \text{at} \quad \eta = \eta_\infty, \end{aligned} \tag{14}$$

The coefficients in Equations (12) and (13) are given by

$$\begin{aligned} X_1^i &= f + \left(\frac{1-m}{1+m}\right)\xi f_\xi, \quad X_2^i = -\left(\frac{4m}{m+1}\right)F - \left(\frac{1-m}{1+m}\right)\xi F_\xi, \\ X_3^i &= -\left(\frac{1-m}{1+m}\right)\xi F, \quad X_4^i = \left(\frac{2}{m+1}\right)\lambda, \\ X_5^i &= -\left(\frac{2m}{m+1}\right)(1+F^2) - \left(\frac{1-m}{m+1}\right)\xi F F_\xi, \\ Y_1^i &= Pr\left[f + \left(\frac{1-m}{1+m}\right)\xi f_\xi\right], \quad Y_2^i = -Pr\left(\frac{1-m}{m+1}\right)\xi F, \\ Y_3^i &= -Pr\left(\frac{1-m}{1+m}\right)\xi G_\xi, \quad Y_4^i = -Pr\left(\frac{1-m}{m+1}\right)\xi F G_\xi. \end{aligned}$$

At each iteration step, the sequence of linear partial differential equations (12) and (13) were expressed in difference form using central difference scheme in the η-direction and backward difference scheme in ξ-direction. The resulting difference equations were then reduced to a system of linear algebraic equations with a block tri-diagonal structure which is solved by using Varga algorithm (Varga, 2000).

To ensure the convergence of the numerical solution to the exact solution, the step sizes $\Delta\eta$ and $\Delta\xi$ have been optimized and the results presented here are independent of the step sizes at least upto the fourth decimal place. The step sizes $\Delta\eta$ and $\Delta\xi$ have been taken as 0.01 and 0.02, respectively. A convergence criteria based on the relative difference between the current and previous iterative values of the velocity and temperature gradients at the wall are employed. When the difference reaches less than 10^{-4}, the solution is assumed to have converged and the iterative process is terminated.

4. Results and discussions

Computations have been carried out for various values of $Pr(0.7 \leq Pr \leq 7.0)$ and $A(-1.2 \leq A \leq 1.2)$. In all numerical computation m is taken 1/2 so that the buoyancy parameter λ becomes a constant and value of λ is in the range $(0 \leq \lambda \leq 7)$. Further, the edge of the boundary layer η_∞ is taken between 3 and 5 depending on the values of parameters. In order to verify the correctness of the procedure, solutions have been obtained for $\xi = 0$, $\lambda = 0$ and $m = 0$ to compare the velocity and temperature profiles (F and G) with those of Kumari *et al.* (1989) for different values of Prandtl number, $Pr = 0.733$ and 6.7. Results are also compared for various values of Prandtl numbers with those of Hering and Grosh (1963) and Himasekhar *et al.* (1989). The results are found in an excellent agreement and only some of the comparisons are shown in Figure 2 to brief the manuscript.

The effects of buoyancy parameter λ, the axial distance ξ and Prandtl number Pr on velocity and temperature profiles (F, G) are displayed in Figures 3-5. Also, the effects of λ and Pr on the skin friction and heat transfer coefficients $(Re_x^{1/2}C_f, Re_x^{-1/2}Nu)$ are presented in Figures 6 and 7. The action of the buoyancy force shows the overshoot in the velocity profiles (F) near the wall for lower Prandtl number ($Pr = 0.7$) but for higher Prandtl number ($Pr = 7.0$) the velocity overshoot in F is not observed as shown in Figure 3. The magnitude of the overshoot increases with buoyancy parameter λ. The reason is that the buoyancy force (λ) effect is larger in a low Prandtl number fluid

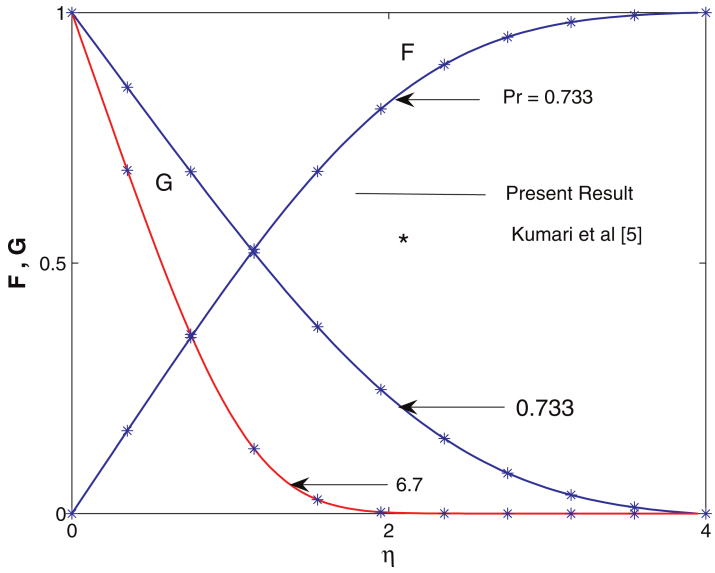

Figure 2.
Comparison of velocity and temperature profiles (F, G) with those of Kumari *et al.* (1989) when $\xi = 0$, $\lambda = 0$ and $m = 0$

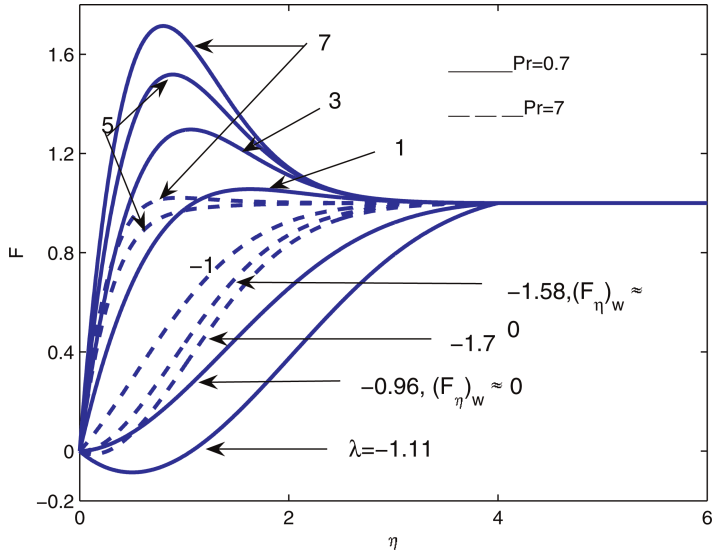

Figure 3.
Effects of λ and Pr on F at $\xi = 0.5$ when $A = 0.2$ and $m = 1/2$

($Pr = 0.7$, air) due to low viscosity of the fluid which enhances the velocity within the boundary layer as the assisting buoyancy force acts like a favorable pressure gradient and the velocity overshoot occurs. For higher Prandtl number fluid ($Pr = 7.0$, water) the velocity overshoot is not present because higher Prandtl number fluid implies more viscous fluid which makes it less sensitive to the buoyancy parameter λ. It is interesting to notice in Figure 3 that at $\xi = 0.5$, for buoyancy opposing flow, i.e. for negative values of buoyancy parameter λ,($\lambda < 0$), the reverse flow starts at $\lambda = -1.58$, for $Pr = 7.0$ (water) and at $\lambda = -0.96$, for $Pr = 0.7$ (air). The buoyancy opposing force reduces the velocity near the wall subsequently as the buoyancy parameter λ decreases further and the fluid flows backward near the wall in a small region as can be seen in Figure 3 for $\lambda = -1.11$ when $Pr = 0.7$ and for $\lambda = -1.7$ when $Pr = 7.0$. The effect of λ is comparatively less on the temperature profiles (G) as shown in Figure 4. Moreover, Figure 4 shows that the increase of Prandtl number Pr results into thinner thermal boundary layer as the higher Prandtl number fluid has a lower thermal conductivity.

Figure 5 shows that due to the increase in axial distance ξ, the steepness in both the velocity and temperature profiles (F, G) near the wall increases and consequently reduce the thicknesses of both the velocity and thermal boundary layers. Further, it may be pointed out that the magnitude of the velocity overshoot slightly decreases with the increase of ξ as can be seen in Figure 5. Thus for the increase of ξ, i.e., at a distant axial location, the effect of buoyancy parameter λ on velocity profiles (F) is small so that it does not cause the velocity profiles to increase the magnitude of overshoots further in buoyancy aided flows. Results presented in Figures 6 and 7 indicate that the skin friction and heat transfer coefficients ($C_f Re_x^{1/2}, NuRe_x^{-1/2}$) increase with the increase of buoyancy parameter (λ). The physical reason is that the positive buoyancy force (λ) implies favorable pressure gradient and the fluid gets accelerated which results in thinner momentum and thermal boundary layers. Consequently, the skin friction ($C_f Re_x^{1/2}$) and the Nusselt number ($NuRe_x^{-1/2}$) also increase with the increase of λ at any ξ as shown in Figures 6 and 7. For example for $Pr = 0.7, A = 1$ at $\xi = 0.5$, the

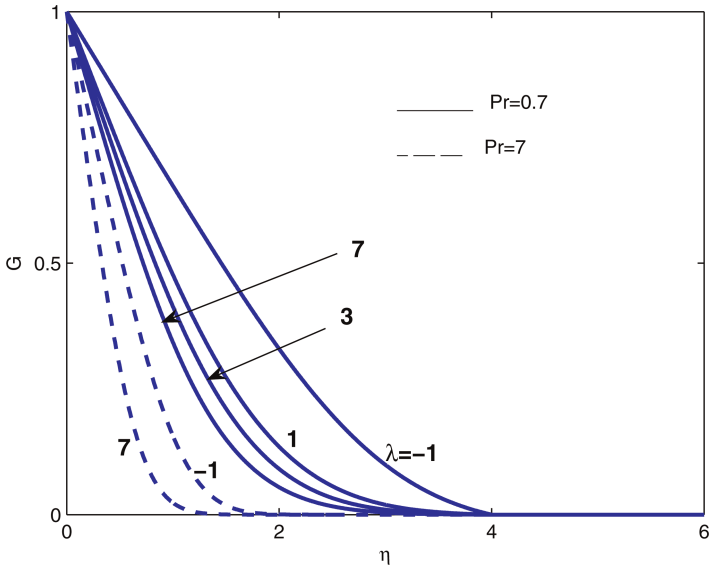

Figure 4.
Effects of λ and Pr on G at $\xi = 0.5$ when $A = 0.2$ and $m = 1/2$

percentage increase in $C_f Re_x^{1/2}$ and $NuRe_x^{-1/2}$ for the increase of λ from 1 to 5 are, approximately, 43 and 5 per cent, respectively.

The effect of surface mass transfer parameter A ($A > 0$ or $A < 0$) on the velocity and temperature profiles (F, G) for $Pr = 0.7$ and $\xi = 1$ are presented in Figure 8. In addition, Figures 9 and 10 display the effect of A on skin friction and heat transfer coefficients ($C_f Re_x^{1/2}$, $NuRe_x^{-1/2}$) with the increase of ξ from 0 to 1. Figures 9 and 10 show that for all ξ, both skin friction and heat transfer coefficients ($C_f Re_x^{1/2}$, $NuRe_x^{-1/2}$) increase with suction ($A > 0$) but decrease with the increase of injection ($A < 0$). In case of injection, the fluid is entered into the boundary layer from the surface causing

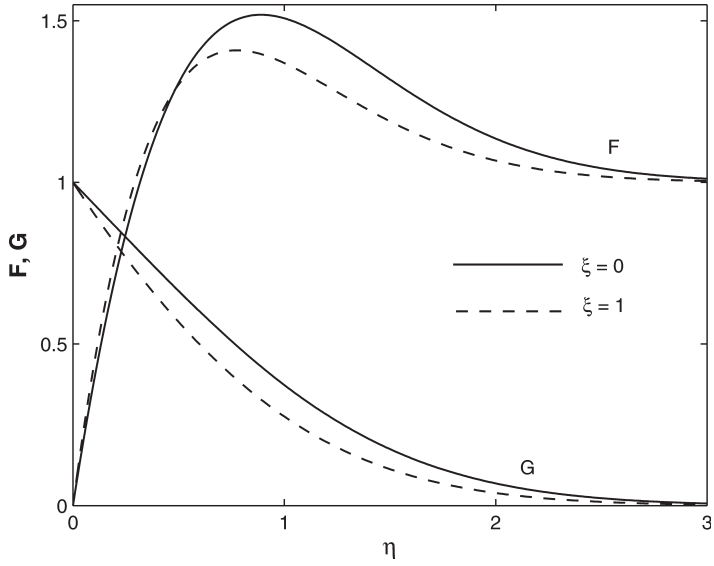

Figure 5.
Effect of ξ on F and G when $Pr = 0.7$, $A = 1$, $\lambda = 5$ and $m = 1/2$

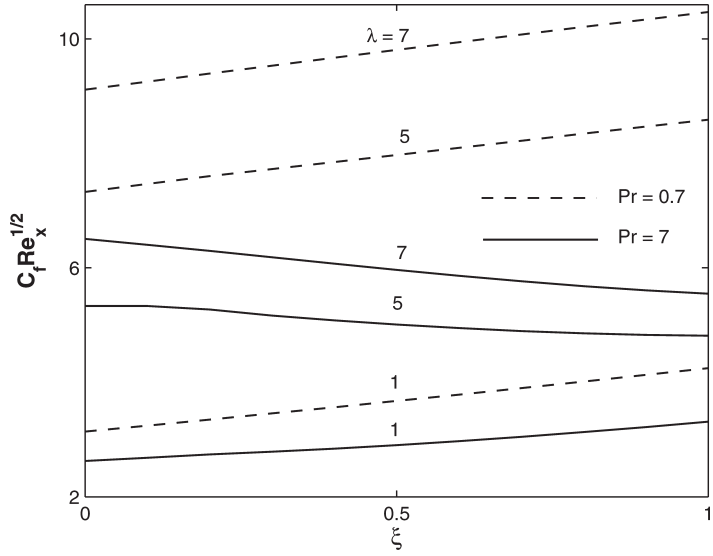

Figure 6.
Effects of λ and Pr on $C_f Re_x^{1/2}$ when $Pr = 0.7$, $A = 1$ and $m = 1/2$

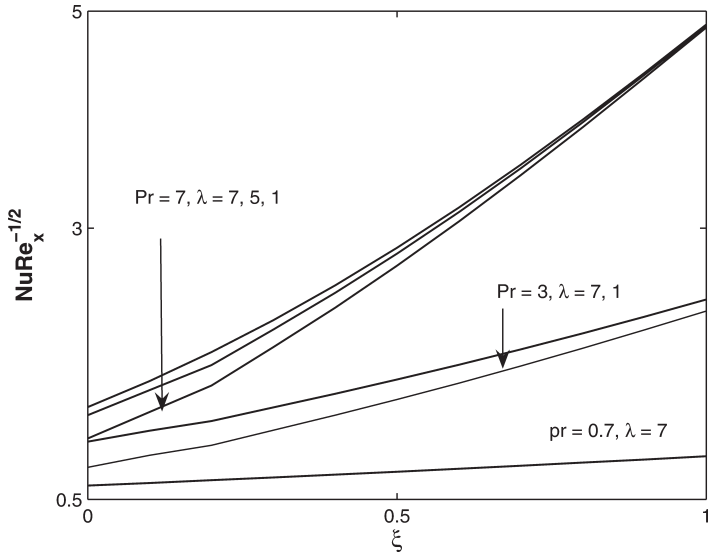

Figure 7.
Effects of λ and Pr on $NuRe_x^{-1/2}$ when $Pr = 0.7$, $A = 1$ and $m = 1/2$

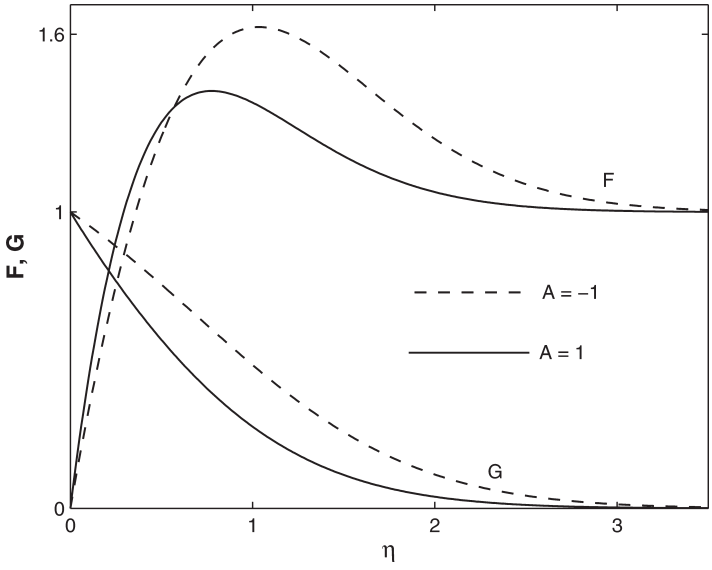

Figure 8.
Effect of A on F and G when $\lambda = 5$, $Pr = 0.7$, $\xi = 1$ and $m = 1/2$

reduction in velocity gradient as it tries to maintain the same velocity over a very small region near the surface and the effect is reverse in case of suction. For example, for $\mathrm{Pr} = 0.7$, $\xi = 1$ both $C_f Re_x^{1/2}$ and $NuRe_x^{-1/2}$ increase, approximately, by 36 and 63 per cent, respectively, with the increase of suction from $A = 0$ to $A = 1$. On the other hand, for $Pr = 0.7$ and $\xi = 1$ due to the increase of injection from $A = 0$ to $A = -1$ both $C_f Re_x^{1/2}$ and $NuRe_x^{-1/2}$ decrease, approximately, by 28 and 47 per cent,

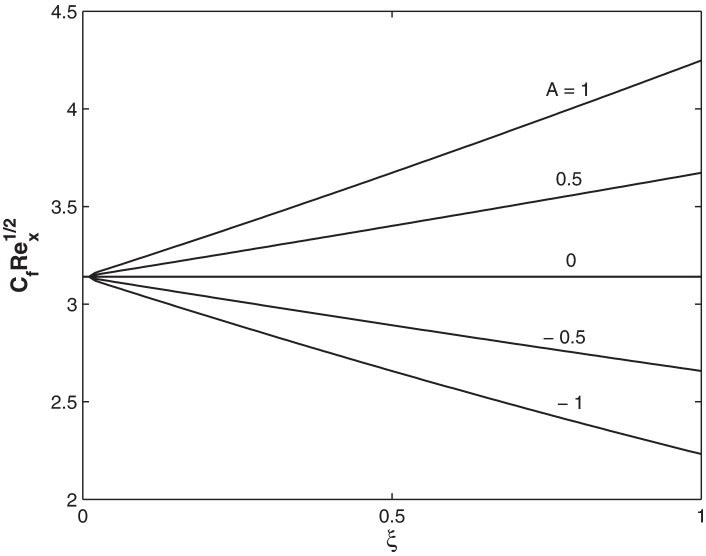

Figure 9.
Effect of A on $C_f Re_x^{1/2}$ when $Pr = 0.7$, $\lambda = 1$ and $m = 1/2$

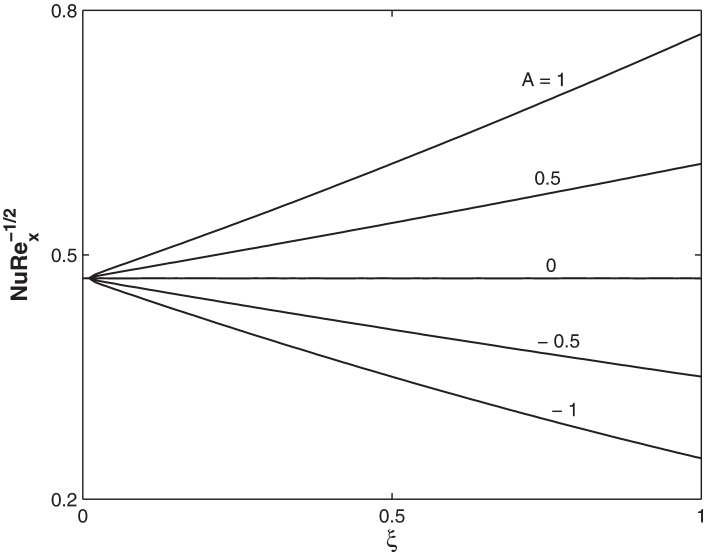

Figure 10.
Effect of A on $NuRe_x^{-1/2}$ when $Pr = 0.7$, $\lambda = 1$ and $m = 1/2$

respectively. It may be noted from Equation (9) that at $\xi = 0$, surface mass transfer distribution f_w is independent of A and $f_w = 0$ for all values of A. Thus, the results presented in Figures 9 and 10 display that all lines are converging to a point at $\xi = 0$. Graphs for the velocity and temperature profiles (F, G) vs η in Figure 8 shows that the injection $(A < 0)$ causes a decrease in the steepness of the profiles F and G near the wall but steepness of the profiles (F, G) increase with suction.

5. Conclusions

Results indicate that the buoyancy force (λ) enhances the skin friction coefficient and Nusselt number. In the buoyancy aiding flow ($\lambda > 0$), the velocity profiles exhibit velocity overshoot for lower Prandtl number. Further, the buoyancy parameter (λ) and injection parameter ($A < 0$) tend to increase its magnitude but the suction parameter ($A > 0$) and axial distance ξ tend to reduce the magnitude of the velocity overshoot. For a fixed buoyancy force, the Nusselt number increases with Prandtl number but the skin friction coefficient decreases. In fact, the increase in Prandtl number causes a significant reduction in the thickness of thermal boundary layer. As expected, both skin friction and heat transfer coefficients increase with suction but decrease with the increase of injection. Moreover, it is noted that the suction parameter ($A > 0$) and the axial distance steepen both the velocity and temperature profiles, but injection ($A < 0$) does the reverse.

References

Anwar Hossain, Md. and Rama Subba Reddy Gorla (2006), "Effect of viscous dissipation on mixed convection flow of water near its density maximum in a rectangular enclosure with isothermal wall", *International Journal of Numerical Methods for Heat and Fluid Flow*, Vol. 16, pp. 5-17.

Bejan, A. (2004), *Convection Heat Transfer*, John Wiley & Sons, Inc., New York, NY.

Bellman, R.E. and Kalaba, R.E. (1965), *Quasilinearization and Non-Linear Boundary Value Problems*, American Elsevier Publishing Co. Inc., New York, NY.

Cruchaga, M. and Celentano, D. (2003), "Modelling natural and mixed convection in obstructed channels", *International Journal of Numerical Methods for Heat and Fluid Flow*, Vol. 13, pp. 57-85.

Daskalakis, J.E. (1993), "Mixed free and forced convection in the incompressible boundary layer along a rotating vertical cylinder with fluid injection", *International Journal of Energy Research*, Vol. 17, pp. 689-95.

Dijk, P.E., Janse, A.M.C., Kuipers, J.A.M. and van Swaaij, W.P.M. (2001), "Hydrodynamics of liquid flow in a rotating cone", *International Journal of Numerical Methods for Heat and Fluid Flow*, Vol. 11, pp. 386-412.

Hering, R.G. and Grosh, R.J. (1963), "Laminar combined convection from a rotating cone", *Transactions: ASME Journal of Heat Transfer*, Vol. 85, pp. 29-34.

Himasekhar, K., Sarma, P.K. and Janardhan, K. (1989), "Laminar mixed convection froma vertical rotating cone", *International Communications in Heat and Mass Transfer*, Vol. 16, pp. 99-106.

Hossain, M.A., Paul, S.C. and Manlal, A.C. (2002), "Natural convection flow along a vertical circular cone with uniform surface temperature and surface heat flux in a thermally stratified medium", *International Journal of Numerical Methods for Heat and Fluid Flow*, Vol. 12, pp. 290-305.

Kumari, M., Pop, I. and Nath, G. (1989), "Mixed convection along a vertical cone", *International Communications in Heat and Mass Transfer*, Vol. 16, pp. 247-55.

Lok, Y.Y., Amin, N., Campean, D. and Pop, I. (2005), "Steady mixed convection flow of amicropolar fluid near the stagnation point on a vertical surface", *International Journal of Numerical Methods for Heat and Fluid Flow*, Vol. 15, pp. 654-70.

Mahmood, T. and Merkin, J.H. (1988), "Mixed convection on a vertical circular cylinder", *Journal of Applied Mathematics and Physics (ZAMP)*, Vol. 39, pp. 186-203.

Nazar, R., Amin, N. and Pop, I. (2003), "Mixed convection boundary layer flow from a horizontal circular cylinder in micropolar fluids: case of constant wall temperature", *International Journal of Numerical Methods for Heat and Fluid Flow*, Vol. 13, pp. 86-109.

Pop, I. and Ingham, D.B. (2001), *Convective Heat Transfer: Mathematical and Computational Modelling of Viscous Fluids and Porous Media*, Pergamon, Oxford.

Pop, I., Grosan, T. and Kumari, M. (2003), "Mixed convection along a vertical cone for fluids of any Prandtl number: case of constant wall temperature", *International Journal of Numerical Methods for Heat and Fluid Flow*, Vol. 13, pp. 815-29.

Pop, I., Kumari, M. and Nath, G. (1989), "Combined free and forced convection along rotating cylinder", *International Journal of Engineering Science*, Vol. 27, pp. 193-202.

Raji, A. and Hasnaoui, M. (2000), "Mixed convection heat transfer in ventilated cavities withopposing and assisting flows", *International Journal of Numerical Methods for Heat and Fluid Flow*, Vol. 17, pp. 556-72.

Rama Subba Reddy Gorla, Slaouti, A. and Takhar, H.S. (1998), "Free convection in micropolar fluids over a uniformly heated vertical plate", *International Journal of Numerical Methods for Heat and Fluid Flow*, Vol. 8, pp. 504-18.

Schlichting, H. (2000), *Boundary Layer Theory*, Springer, New York, NY.

Singh, P.J. and Roy, S. (2007), "Unsteady mixed convection flow over a vertical cone due to impulsive motion", *International Journal of Heat and Mass Transfer*, Vol. 50, pp. 949-59.

Varga, R.S. (2000), *Matrix Iterative Analysis*, Springer, New York, NY.

Wang, C.Y. (1990), "Boundary layer on a rotating cones, disc, axisymmetric surfaces with concentrated heat sources", *Acta Mechanica*, Vol. 81, pp. 245-51.

Yih, K.A. (1999), "Mixed convection about a cone in a porous medium: the entire region", *International Communications in Heat and Mass Transfer*, Vol. 26, pp. 1041-50.

Corresponding author
R. Ravindran can be contacted at: Ravindran.Ramalingam@wits.ac.za